Quantitative modeling of fluorescent emission in photonic crystals

Johannes Gutmann,[1,*] Hans Zappe,[2] and Jan Christoph Goldschmidt[1,3]
[1]*Fraunhofer Institute for Solar Energy Systems ISE, Heidenhofstraße 2, 79110 Freiburg, Germany*
[2]*Gisela and Erwin Sick Chair of Micro-optics, Department of Microsystems Engineering - IMTEK, University of Freiburg, Georges-Köhler-Allee 102, 79110 Freiburg, Germany*
[3]*Department of Physics, Imperial College, London SW7 2AZ, United Kingdom*
(Received 14 June 2013; revised manuscript received 23 October 2013; published 13 November 2013; publisher error corrected 20 November 2013)

Photonic crystals affect the photon emission of embedded emitters due to an altered local density of photon states (LDOS). We review the calculation of the LDOS from eigenmodes in photonic crystals and propose a rate equation model for fluorescent emitters to determine the changes in emission induced by the LDOS. We show how to calculate the modifications of three experimentally accessible characteristics: emission spectrum (spectral redistribution), emitter quantum yield, and fluorescence lifetime. As an example, we present numerical results for the emission of the dye Rhodamine B inside an opal photonic crystal. For such photonic crystals with small permittivity contrast, the LDOS is only weakly modified, resulting in rather small changes. We point out that in experiments, however, usually only part of the emitted light is detected, which can have a very different spectral distribution (e.g., due to a photonic band gap in the direction of detection). We demonstrate the calculation of this detected spectrum for a typical measurement setup. With this reasoning, we explain the previously not fully understood experimental observation that strong spectral modifications occurred, while at the same time only small changes in lifetime were found. With our approach, the mentioned effects can be quantitatively calculated for fluorescent emitters in any photonic crystal.

DOI: 10.1103/PhysRevB.88.205118 PACS number(s): 42.70.Qs, 78.55.−m, 33.50.−j, 42.50.Ct

I. INTRODUCTION

In the 1940's, Purcell pointed out that the rate of spontaneous emission is affected by the light source's environment, namely, inside resonant cavities.[1] It was the introduction of photonic crystals 40 years later[2,3] that has drawn particular attention to this phenomenon. Being nanostructures with a periodic modulation of the relative permittivity ϵ, photonic crystals offer fascinating means for the manipulation of light.

Analogous to solid state physics, where electrons face a periodic potential, one can derive the photon dispersion relation $\omega(\boldsymbol{k})$ that relates the frequency ω and the wave vector $\boldsymbol{k}$. While in homogeneous dielectric media the dispersion of plane waves is simply $\omega(\boldsymbol{k}) = c|\boldsymbol{k}|/\sqrt{\epsilon}$, it can become strongly nonlinear in photonic crystals: photons with certain energies may not be allowed to propagate in certain directions, which gives rise to photonic band gaps.

Photonic crystals strongly modify the emission of embedded light sources as already pointed out in the pioneering works of Yablonovitch[2] and Bykov.[4] This influence can be understood in terms of the spontaneous emission probability P_{if}, which in the weak-coupling regime depends on the local density of photon states (LDOS) $\rho(\boldsymbol{r},\omega)$ as stated by Fermi's golden rule:[5]

$$P_{\mathrm{if}}(\boldsymbol{r}) = \frac{2\pi}{\hbar}|\langle f|H_{\mathrm{int}}|i\rangle|^2\rho(\boldsymbol{r},\omega_{\mathrm{if}}), \tag{1}$$

where H_{int} denotes the interaction part of the Hamiltonian coupling the emitter to the field. Consequently, the probability for the radiative transition of electrons from electronic state $|i\rangle$ to $\langle f|$ is proportional to $\rho(\boldsymbol{r},\omega_{\mathrm{if}})$, as a photon with energy $\hbar\,\omega_{\mathrm{if}}$ can be emitted only if there is an appropriate photon state it can populate.

In homogeneous media, the LDOS is a quadratic function of the frequency ω, independent of the position $\boldsymbol{r}$. As a result of the linear dispersion relation, the LDOS is proportional to $\sqrt{\epsilon}$. In photonic crystals, however, the LDOS can be modified due to flat bands and band gaps, for example.

The LDOS of a certain structure can be obtained using different approaches. For ideal, i.e., infinite photonic crystals the LDOS can be calculated efficiently from eigenmode calculations,[6–9] which we use in this work. Finite and nonperiodic structures can be treated with the Green's function approach,[10–13] the transfer matrix,[14] and scattering matrix method[15] or using finite-difference time-domain (FDTD) calculations.[16,17]

It was shown that the LDOS can differ strongly from the *total* density of photon states (DOS) that is independent of $\boldsymbol{r}$. The LDOS strongly depends on the actual emitter position[6,9] and its dipole orientation.[13]

In experiments, various light sources (rare-earth ions,[18,19] organic dye molecules,[8,20,21] semiconductor quantum dots,[22–25] and quantum wells[26]) have been embedded in different photonic crystals to study the emission properties. Further, biological samples have been investigated, such as wings of butterflies that feature fluorophores within photonic structure.[15,27]

The shape of the measured emission spectra was found to be strongly modified. This effect was attributed to suppression of emission within photonic band gaps and enhancement at band edges. For the fluorescence lifetime, however, only little effect was observed in time-resolved measurements in "weak" photonic crystals, featuring incomplete, i.e., not omnidirectional band gaps (e.g., opals with small permittivity contrast).[8,20,21] In contrast, photonic crystals with complete band gaps (e.g., woodpile or diamond structures from high-permittivity materials) significantly influenced the decay time when emitters were embedded.[24,25]

The experimental results, however, have been compared only qualitatively to theoretical LDOS calculations, e.g., by

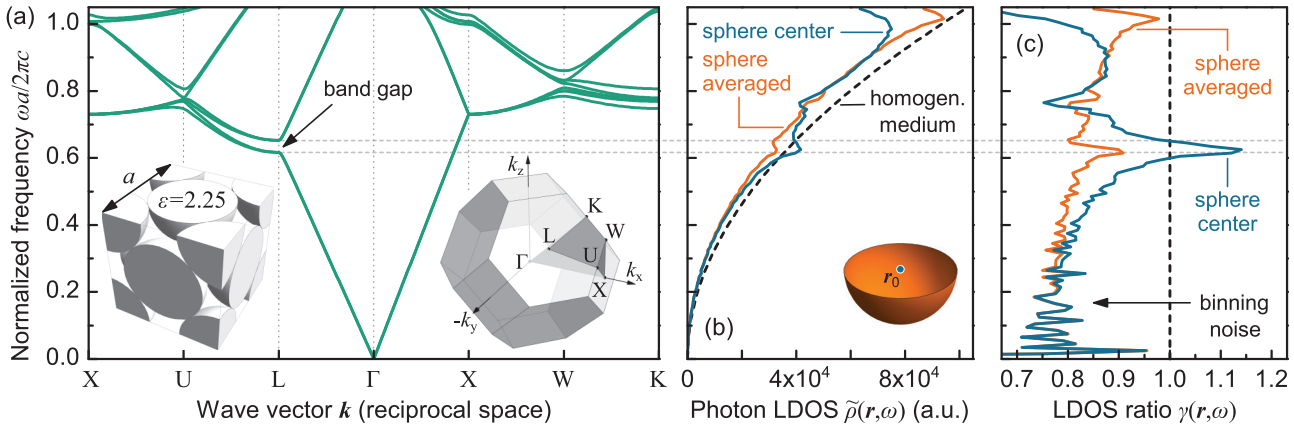

FIG. 1. (Color online) The dispersion relation $\omega(\boldsymbol{k})$ of an opal photonic crystal (fcc lattice of dielectric spheres, left inset) features a photonic band gap in the L direction (a). The different crystallographic orientations are indicated in the right inset that illustrates the first Brillouin zone. The local density of photon states at the sphere center ($\boldsymbol{r}_0$) and averaged over the whole sphere is shown in (b), confirming the strong influence of the emitter position. The ratio to the LDOS in homogeneous medium determines the change in radiative transition probabilities. Here, the LDOS is enhanced at the lower band edge of the band gap (c).

comparing the emission spectrum with the LDOS spectrum.[8] In this work, we present a treatment of emission inside photonic crystals that quantifies the impact of the changed LDOS onto the emitter. This allows for calculating experimentally observable characteristics, such as the emission spectrum, the emitter quantum yield, and the fluorescence lifetime. Thereby we also consider the measured spectrum observed outside the photonic crystal. It may differ from the actual emission spectrum as only part of the emitted light can couple out and falls on the detector.

In the first part, we recall the calculation of electromagnetic eigenmodes in photonic crystals and derive the LDOS. Second, we propose a rate equation model for fluorescent emitters to model its emission. It is particularly interesting to study fluorescent emitters such as organic dyes: they typically exhibit broad emission spectra compared to the sharp features in the LDOS of photonic crystals. When emission at a certain frequency is suppressed, the photon can still be emitted through other decay channels at different frequencies (spectral redistribution). In the third part, we calculate the influence of the photonic crystal on the emitter in terms of (detected) emission spectrum, emitter quantum yield, and fluorescent lifetime.

Our treatment is quite general and can be applied to arbitrary photonic crystals. To show results, for an example, however, we present a case study using an opal photonic crystal, which is a close-packed, face-centered cubic (fcc) arrangement of spheres, with $\epsilon_{\text{spheres}} = 2.25$ (e.g., polymer) and $\epsilon_{\text{voids}} = 1$ (air), i.e., a weak photonic crystal. Its fcc unit cell and the corresponding first Brillouin zone (FBZ) are shown in the insets of Fig. 1(a). As an example for a fluorescent emitter, we model the properties of the rhodamine B dye, for which embedding inside polymer spheres was already shown experimentally.[28] To match the emission spectrum of the dye with the opal's first band gap, we chose the unit cell size $a = 377.6$ nm (sphere diameter of 267 nm).

II. LDOS CALCULATIONS

In the following, the eigenmodes of an infinite and periodic photonic crystal are calculated to obtain the LDOS, which is used as an input to the emitter model. If other methods are used to compute the LDOS, it is essential to use full three-dimensional calculations that include all possible modes an emitter can emit.

Starting from Maxwell's equations for nonmagnetic, charge-free, and dispersionless materials [$\mu = \rho = 0$, $\boldsymbol{j} = \boldsymbol{0}$, $\epsilon \neq \epsilon(\omega)$] with an harmonic ansatz for the fields [$\boldsymbol{E}(\boldsymbol{r},t) = \boldsymbol{E}(\boldsymbol{r})\, e^{-i\omega t}$, $\boldsymbol{H}$ analogous], we obtain the wave equation for the H field:

$$\nabla \times \left(\frac{1}{\epsilon(\boldsymbol{r})} \nabla \times \boldsymbol{H}(\boldsymbol{r}) \right) = \left(\frac{\omega}{c} \right)^2 \boldsymbol{H}(\boldsymbol{r}), \tag{2}$$

which is a Hermitian eigenvalue problem with the eigenvalue $(\omega/c)^2$ and the field $\boldsymbol{H}(\boldsymbol{r})$ as the eigenvector.[29]

Due to the photonic crystal's discrete translational symmetry $\epsilon(\boldsymbol{r}) = \epsilon(\boldsymbol{r} + \boldsymbol{R})$ (with lattice vector $\boldsymbol{R}$ as a linear combination of the primitive lattice vectors), the Bloch theorem yields

$$\boldsymbol{H}_{n,\boldsymbol{k}}(\boldsymbol{r}) = e^{i\boldsymbol{k}\boldsymbol{r}} \boldsymbol{u}_{n,\boldsymbol{k}}(\boldsymbol{r}) \tag{3}$$

as solutions to Eq. (2) with the function $\boldsymbol{u}_{n,\boldsymbol{k}}(\boldsymbol{r}) = \boldsymbol{u}_{n,\boldsymbol{k}}(\boldsymbol{r} + \boldsymbol{R})$ being periodic on the crystal lattice. In this way, the wave vector $\boldsymbol{k}$ and the band index n are introduced. Inserting Eq. (3) in Eq. (2) results again in a Hermitian eigenvalue problem that can be solved numerically using the plane-wave expansion method, as described in Ref. 30.

For $\boldsymbol{k}$-vector values along certain directions of the reciprocal space, the associated modes with frequencies ω can be computed to obtain the dispersion relation $\omega(\boldsymbol{k})$. The dispersion relation for our opal example is shown in Fig. 1(a). The opal features a band gap in crystallographic L direction ($\langle 111 \rangle$), i.e., there are no solutions $\boldsymbol{H}_{n,\boldsymbol{k}}(\boldsymbol{r})$ to Eq. (2), with $\boldsymbol{k}$ in this direction, that have frequencies inside the gap.

The LDOS $\rho(\boldsymbol{r},\omega)$ is defined as[6]

$$\rho(\boldsymbol{r},\omega) = \sum_n \int_{\text{FBZ}} |\boldsymbol{E}_{n,\boldsymbol{k}}(\boldsymbol{r})|^2 \delta(\omega - \omega_{n,\boldsymbol{k}}) d\boldsymbol{k}, \tag{4}$$

which can be understood in terms of counting all states in the FBZ with a certain frequency, weighted with each

individual field distribution. This introduces the spatial dependence of the LDOS, opposed to the total DOS $\rho(\omega) = \sum_n \int_{\mathrm{FBZ}} \delta(\omega - \omega_{n,\boldsymbol{k}})d\boldsymbol{k}$, which counts all states with same weights. For the emission process, however, the LDOS is the relevant quantity rather than the total DOS: given a mode with a field pattern being zero at a certain position (e.g., due to a node), an emitter at that position cannot excite this mode.

The dipole orientation of an emitter is neglected here as we assume emission from an ensemble with randomly oriented dipole moments. However, the influence of the emitter orientation could be easily implemented following the analysis in Ref. 13.

To calculate $\rho(\boldsymbol{r},\omega)$ from a finite set of eigenmodes, one could linearly interpolate the dispersion relation using the tetrahedron method.[6,31,32] Here, we employed the histogramming method[9] as it is more comprehensible and allows calculating the *fractional* LDOS (FLDOS) as explained later (Sec. IV B). Thus we approximate Eq. (4) by the sum

$$\rho(\boldsymbol{r},\omega) \approx \tilde{\rho}(\boldsymbol{r},\omega) = \sum_n \sum_{\boldsymbol{k}\in\mathfrak{K}_{n,\omega}} \left|\boldsymbol{E}_{n,\boldsymbol{k}_j}(\boldsymbol{r})\right|^2 \tag{5}$$

$$\text{with} \quad \mathfrak{K}_{n,\omega} = \left\{\boldsymbol{k}_j \middle| \omega - \Delta\omega/2 \leqslant \omega_{n,\boldsymbol{k}_j} < \omega + \Delta\omega/2\right\} \tag{6}$$

and the binning width $\Delta\omega$.

Rather than calculating only some modes along certain directions [as for the dispersion relation in Fig. 1(a)], we need to consider all FBZ wave vectors $\boldsymbol{k}_j$ on an equidistant grid in $\boldsymbol{k}$ space. It is possible to use only the wave vectors of an irreducible symmetry element of the FBZ [such as the one indicated in the inset of Fig. 1(a)]. However, this requires an additional transformation as the fields do not necessarily exhibit the same symmetry as the $\boldsymbol{k}$ vectors.[7] In this work, we calculated all wave vectors of the whole FBZ, simplifying the evaluation of LDOS and FLDOS.

The resolution and accuracy of $\tilde{\rho}(\boldsymbol{r},\omega)$ due to binning noise depend on the grid spacing Δk in $\boldsymbol{k}$ space. Here, we calculated all modes within the whole FBZ (with $\Delta k = 0.01/a$) up to the eighth band to obtain all states with $\omega < 1$ ($\Delta\omega = 0.01\ 2\pi c/a$).

To compare the LDOS $\tilde{\rho}^{\mathrm{PC}}(\boldsymbol{r},\omega)$ in a photonic crystal with the reference case of homogeneous media, we calculated the LDOS ratio

$$\gamma(\boldsymbol{r},\omega) = \frac{\tilde{\rho}^{\mathrm{PC}}(\boldsymbol{r},\omega)}{\tilde{\rho}^{0}(\boldsymbol{r},\omega)}, \tag{7}$$

where $\tilde{\rho}^{0}(\boldsymbol{r},\omega)$ is the corresponding "binned" LDOS in a homogeneous medium with relative permittivity $\epsilon = \epsilon(\boldsymbol{r})$ given by[33]

$$\tilde{\rho}^{0}(\boldsymbol{r},\omega) = \int_{\omega-\Delta\omega/2}^{\omega+\Delta\omega/2} \rho^{0}(\boldsymbol{r},\omega)d\omega = \frac{8\pi\sqrt{\epsilon}\,\Delta\omega}{c^3\Delta k^3}\left(\omega^2 + \frac{\Delta\omega^2}{12}\right). \tag{8}$$

In Fig. 1(b), we plot the LDOS of our opal for an emitter in the sphere center ($\boldsymbol{r}_0$) as well as averaged over all positions inside a sphere (a configuration that might be realized in experiments). The results confirm that the LDOS strongly depends on $\boldsymbol{r}$. Comparing with the homogeneous LDOS, the LDOS ratio lies below one for most frequencies considered here, indicating rather a suppression than an enhancement [see Fig. 1(c)].[34]

In general, the variations in the LDOS are quite small due to the low permittivity contrast. Although the opal features a band gap in one direction, there are many states with $\boldsymbol{k}$ vectors in other directions that have frequencies inside the gap. Thus the LDOS does not drop to zero within the band gap but shows relatively small variations. In both cases, however, the LDOS is largest at the lower band edge. This effect can be understood with the shift of the band gap towards higher frequencies as wave vectors tilt from L to U direction, reducing the number of modes with frequencies near the upper band edge.

III. EMITTER MODEL

To calculate the influence of the photonic crystal, we propose in the following a rate equation model for fluorescent emitters such as the organic dye rhodamine B in our case study. This allows the quantitative calculation of the emission modifications in terms of emission spectrum, emitter quantum yield, and fluorescent lifetime.

Fluorescent molecules feature rather complex energetic structures that can be described by an electronic ground state and one (or more) excited states [see Fig. 2(a)]. These electronic states are split up into a number of vibrational energy levels, which are further subdivided into rotational energy levels of the molecule. Therefore absorption and emission spectra are typically quite broad.

Electrons being absorbed from the ground state to one of the vibrational levels of an excited state undergo vibrational relaxations to the lowest level of the first excited state. From this level, electrons can radiatively (or nonradiatively) decay to one of the ground-state levels. Thus most emitted photons have lower energies than the absorbed ones, which is known as the *Stokes shift*.

As the vibrational transitions $\sim 10^{-12}$ s are much faster than the radiative decay $\sim 10^{-9}$ s, emission can be assumed to originate only from the lowest level of the excited state.[35] For our treatment of fluorescent emission inside photonic crystals,

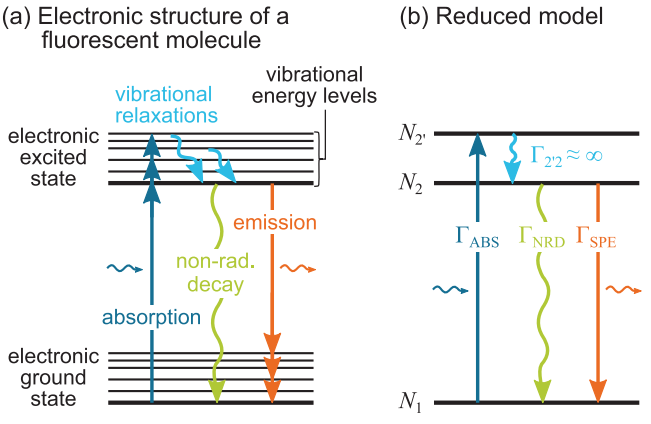

FIG. 2. (Color online) The electronic structure of fluorescent molecules typically consists of a ground and an excited state, both split up into vibrational levels (a). As a result, absorption and emission spectra are quiet broad. As vibrational relaxations happen very fast, emission originates only from the lowest excited state level. Using appropriate spectral shape functions, we thus model the emitter with two states (b).

we thus reduce the electronic structure to a quasi-two-level model as depicted in Fig. 2(b). The separation of the excited state in state 2 and state 2′ accounts for the Stokes shift. Due to the quasi-instantaneous relaxation (transition rate $\Gamma_{2'2} \approx \infty$), however, all excited emitters are in state 2, thus $N_{2'} = 0$.

To model the spectral widths of absorption and emission we employ "spectral shape functions." They aggregate all transitions to the different energy levels of the ground state (for emission) and of the excited state (for absorption).

Following Einstein's treatment of transition rates, the rate of spontaneous emission Γ_{SPE} of an emitter ensemble is the product of the number of emitters in the excited state N_2 and the transition probability P_{SPE}. This transition probability can be described via

$$P^0_{\mathrm{SPE}} = \int A^0_{21} g^0(\omega) d\omega, \tag{9}$$

where A^0_{21} denotes the corresponding Einstein coefficient. The spectral shape function $g^0(\omega)$ with $\int g^0(\omega)d\omega = 1$ can be implemented analogously to a classical "line-shape function" as $g^0(\omega)$ represents the sum of all transitions to different vibrational and rotational energy levels. The superscript "0" denotes the reference case of emission in a homogeneous material for which $g^0(\omega)$ can be obtained from appropriate photoluminescence measurements, e.g., using a confocal setup to minimize reabsorption artifacts.

Inside photonic crystals, the spontaneous emission probability is modified through the LDOS ratio $\gamma(\boldsymbol{r},\omega)$ according to Fermi's golden rule [see Eq. (1)]:

$$P^{\mathrm{PC}}_{\mathrm{SPE}}(\boldsymbol{r}) = \int A^0_{21} g^0(\omega)\gamma(\boldsymbol{r},\omega)d\omega = \alpha(\boldsymbol{r}) P^0_{\mathrm{SPE}}, \tag{10}$$

where we defined the emission probability enhancement factor $\alpha(\boldsymbol{r}) = \int g^0(\omega)\gamma(\boldsymbol{r},\omega)d\omega$. Note that the emission probability in a photonic crystal depends on the emitter location $\boldsymbol{r}$.

In Eq. (10), we neglect the rather small effects of the photonic crystal on natural broadening and Lamb shift of each individual transition within the emission spectrum as the total spectral shape is typically much broader than these effects.[33] While the function $g^{\mathrm{PC}}(\boldsymbol{r},\omega) = g^0(\omega)\gamma(\boldsymbol{r},\omega)/\alpha(\boldsymbol{r})$ reveals the spectral shape of the emitted spectrum, the spontaneous emission rate $\Gamma^{\mathrm{PC}}_{\mathrm{SPE}}(\boldsymbol{r}) = N^{\mathrm{PC}}_2 P^{\mathrm{PC}}_{\mathrm{SPE}}(\boldsymbol{r})$ is a measure of the intensity of emission ("number of photons per second"). This rate includes the number of excited emitters N^{PC}_2 that might be different from N^0_2. The steady-state population of the electronic states, however, depends on the rate of absorption $\Gamma_{\mathrm{ABS}} = N_1 B_{12'} u(\omega_{12'})$ (in fact, accounting for the broad absorption spectra and broad-band excitation: $\Gamma_{\mathrm{ABS}} = N_1 \int B_{12'}(\omega)u(\omega)d\omega$).

While the corresponding Einstein coefficient $B_{12'}$ does not change due to LDOS effects, the excitation through the spectral energy density $u(\omega)$ depends on many factors: where does the light come from (e.g., from outside a finite photonic crystal) and how is the electromagnetic field distribution within the photonic crystal as a function of $\boldsymbol{r}$? The modified local spectral energy density $u^{\mathrm{PC}}(\omega,\boldsymbol{r})$ in photonic crystals can be calculated only for a specific geometry, e.g., using numerical methods like finite-difference time domain,[36,37] rigorous coupled wave analysis,[38] or the scattering matrix formalism,[39] which is out of the scope of this paper.

Nonetheless, assuming such calculations yield a local absorption probability enhancement of $\beta(\boldsymbol{r}) = u^{\mathrm{PC}}(\omega_{12'},\boldsymbol{r})/u^0(\omega_{12'})$ [with broad band: $\beta(\boldsymbol{r}) = \int B_{12'}(\omega)u^{\mathrm{PC}}(\omega,\boldsymbol{r})d\omega / \int B_{12'}(\omega)u^0(\omega)d\omega$], we can express the three transition rates of an emitter inside a photonic crystal as

$$\Gamma^{\mathrm{PC}}_{\mathrm{ABS}} = \beta(\boldsymbol{r})\left(N^{\mathrm{PC}}_1 / N^0_1\right)\Gamma^0_{\mathrm{ABS}}, \tag{11}$$

$$\Gamma^{\mathrm{PC}}_{\mathrm{SPE}} = \alpha(\boldsymbol{r})\left(N^{\mathrm{PC}}_2 / N^0_2\right)\Gamma^0_{\mathrm{SPE}}, \tag{12}$$

$$\Gamma^{\mathrm{PC}}_{\mathrm{NRD}} = \left(N^{\mathrm{PC}}_2 / N^0_2\right)\Gamma^0_{\mathrm{NRD}}, \tag{13}$$

where we introduced the nonradiative decay rate $\Gamma_{\mathrm{NRD}} = N_2 P_{\mathrm{NRD}}$, whose transition probability P_{NRD} is assumed to be independent of the photon LDOS as it represent electronic transitions where no photon is emitted (which would require a photon state). As we assume a relatively low spectral energy density (weak-coupling regime), stimulated emission processes are neglected.

Comparing the steady-state rates

$$\Gamma^0_{\mathrm{ABS}} = \Gamma^0_{\mathrm{SPE}} + \Gamma^0_{\mathrm{NRD}}, \tag{14}$$

$$\Gamma^{\mathrm{PC}}_{\mathrm{ABS}} = \Gamma^{\mathrm{PC}}_{\mathrm{SPE}} + \Gamma^{\mathrm{PC}}_{\mathrm{NRD}}$$

$$\Leftrightarrow \beta(\boldsymbol{r})\frac{N^{\mathrm{PC}}_1}{N^0_1}\Gamma^0_{\mathrm{ABS}} = \frac{N^{\mathrm{PC}}_2}{N^0_2}\left(\alpha(\boldsymbol{r})\Gamma^0_{\mathrm{SPE}} + \Gamma^0_{\mathrm{NRD}}\right), \tag{15}$$

we find the change of the ground and excited state populations ($N_{\mathrm{tot}} = N_1 + N_2$ being the total number of emitters):

$$\frac{N^{\mathrm{PC}}_1}{N^0_1} = \frac{1}{\xi(\boldsymbol{r})\left(1 - N^0_1/N_{\mathrm{tot}}\right) + N^0_1/N_{\mathrm{tot}}} \approx 1, \tag{16}$$

$$\frac{N^{\mathrm{PC}}_2}{N^0_2} = \frac{\xi(\boldsymbol{r})}{1 + (\xi(\boldsymbol{r}) - 1)N^0_2/N_{\mathrm{tot}}} \approx \xi(\boldsymbol{r}) \tag{17}$$

$$\text{with} \quad \xi(\boldsymbol{r}) = \frac{\beta(\boldsymbol{r})}{1 + \Phi^0(\alpha(\boldsymbol{r}) - 1)},$$

where we introduced the emitter quantum yield $\Phi^0 = \Gamma^0_{\mathrm{SPE}}/\Gamma^0_{\mathrm{ABS}}$ that is the ratio of emitted photons to absorbed photons. The approximations in Eqs. (16) and (17) correspond to the weak-coupling regime, where $N^0_1 \gg N^0_2$.[40] In fact, the approximations are equal to the zeroth-order Taylor expansion around $N^0_1 = N_{\mathrm{tot}}$ [see Eq. (16)] and $N^0_2 = 0$ [see Eq. (17)].

These results for the populations yield the change in transition rates due to the photonic crystal

$$\Gamma^{\mathrm{PC}}_{\mathrm{ABS}}/\Gamma^0_{\mathrm{ABS}} \approx \beta(\boldsymbol{r}), \tag{18}$$

$$\Gamma^{\mathrm{PC}}_{\mathrm{SPE}}/\Gamma^0_{\mathrm{SPE}} \approx \frac{\alpha(\boldsymbol{r})\beta(\boldsymbol{r})}{1 + \Phi^0(\alpha(\boldsymbol{r}) - 1)}, \tag{19}$$

$$\Gamma^{\mathrm{PC}}_{\mathrm{NRD}}/\Gamma^0_{\mathrm{NRD}} \approx \frac{\beta(\boldsymbol{r})}{1 + \Phi^0(\alpha(\boldsymbol{r}) - 1)}. \tag{20}$$

Note that all three transition rates and also the populations in a photonic crystal are functions of the emitter position $\boldsymbol{r}$, although not explicitly stated.

Hence, the absolute intensity of emission depends on the enhancement of the probabilities of absorption $\beta(\boldsymbol{r})$ and emission $\alpha(\boldsymbol{r})$ as well as on the quantum yield Φ^0 of the emitter. In the absence of nonradiative decay channels ($\Phi^0 = 1$), the rates of both absorption and emission would be enhanced by the same factor $\beta(\boldsymbol{r})$. This factor $\beta(\boldsymbol{r})$ depends on the specific

geometry, the source of excitation and needs to be obtained separately as mentioned above. Independent of the absorption rate [and its modification $\beta(\boldsymbol{r})$], however, we can calculate how many of the absorbed photons are emitted, i.e., the emitter quantum yield inside the photonic crystal Φ^{PC}, as we show in Sec. IV C.

IV. EFFECTS OF THE PHOTONIC CRYSTAL

A. Spectral redistribution (total emission)

As mentioned above, spontaneous emission from emitters with broad emission spectra may be spectrally redistributed as excited state electrons can decay to different ground state levels. Emission at frequencies with a relatively low LDOS ratio is suppressed and instead light is emitted at frequencies with higher LDOS ratios. The spectral distribution of the emitted light can be obtained from the spectral shape functions $g^0(\omega)$ and $g^{\mathrm{PC}}(\boldsymbol{r},\omega)$.

For our opal case study, the spectral shape function $g^0(\omega)$ of Rhodamine B was initially obtained from photoluminescence measurements of a dye-doped polymer film with $\epsilon = 2.25$ (spin-coated on a glass substrate). In this way, the dye molecules experience the same chemical environment as in an opal with spheres made of the same polymer. It is necessary to compare the emission in identical host materials to avoid other, chemical effects that modify the emission.

Based on this $g^0(\omega)$ as an input parameter, the emission spectrum in the photonic crystal was calculated for a dye molecule at the sphere center $\boldsymbol{r}_0$ (see Fig. 3): emission is redistributed from the upper-frequency band edge to the lower-frequency band edge of the gap in L direction due to the elevated LDOS at these wavelengths. However, the effect is rather small as the LDOS in this example features only small variations [see Fig. 1(b)].

The emission spectrum depends on the exact emitter position within the photonic crystal. To model a particular spatial distribution of emitters, e.g., to compare to corresponding experiments, the emission spectrum for each emitter positions needs to be calculated individually. In general, it is not correct to first average the LDOS over all relevant $\boldsymbol{r}$, and to subsequently use this averaged LDOS for further calculations.

Accordingly, the spectral shape $g^{\mathrm{PC}}_{\mathrm{tot}}(\omega)$ of light emitted by many emitters at different $\boldsymbol{r}_i$ is not just the average of their $g^{\mathrm{PC}}(\boldsymbol{r}_i,\omega)$. Instead, $g^{\mathrm{PC}}_{\mathrm{tot}}(\omega)$ is given by the sum of the individual contributions, while considering the local rates $\Gamma^{\mathrm{PC}}_{\mathrm{SPE}}(\boldsymbol{r}_i)$:

$$g^{\mathrm{PC}}_{\mathrm{tot}}(\omega) = s \sum_i g^{\mathrm{PC}}(\boldsymbol{r}_i,\omega)\,\Gamma^{\mathrm{PC}}_{\mathrm{SPE}}(\boldsymbol{r}_i)$$

$$\approx s\,\Gamma^0_{\mathrm{SPE}} \sum_i \frac{g^{\mathrm{PC}}(\boldsymbol{r}_i,\omega)\,\alpha(\boldsymbol{r})\beta(\boldsymbol{r})}{1+\Phi^0(\alpha(\boldsymbol{r})-1)}, \qquad (21)$$

with normalization factor $s = \sum_i \Gamma^{\mathrm{PC}}_{\mathrm{SPE}}(\boldsymbol{r}_i)$. As $g^{\mathrm{PC}}_{\mathrm{tot}}(\omega)$ depend on $\beta(\boldsymbol{r})$, local absorption needs to be considered to obtain the emission spectrum of a group of emitters.

We emphasize that all calculations of this section yield the spectral distribution of all emitted light, independent of its propagation direction. In experiments, this spectrum could be recorded using an integrating sphere, when all modes (even trapped ones) are able to escape from a finite sample, e.g., at the edge faces.

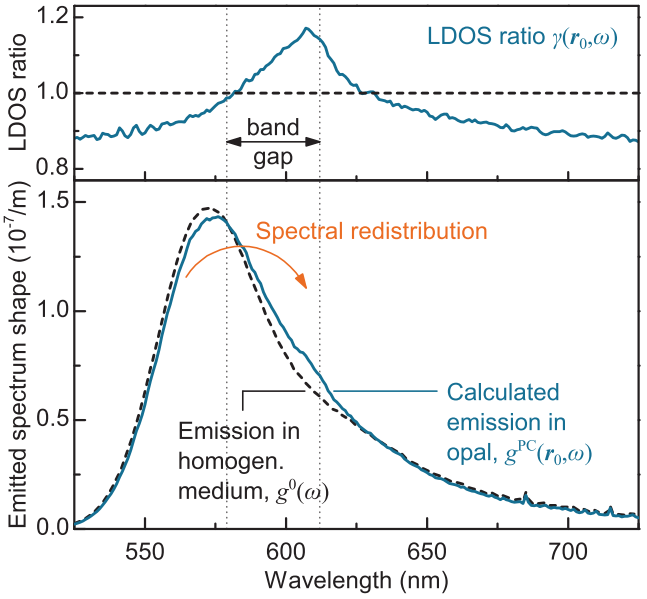

FIG. 3. (Color online) As a results of the modified LDOS inside photonic crystals, emitted light is spectrally redistributed, changing the shape of the emission spectrum. Here, part of the emission of the rhodamine B dye (at $\boldsymbol{r}_0$) is shifted from shorter to longer wavelengths, where the LDOS is enhanced.

In most experiments, however, only part of the emitted light is detected, which explains why previous experimental papers[8,20–22] reported much stronger modifications of the emission spectrum than in our calculation even for structures with permittivity contrast similar to the one modeled by us. To calculate the detected spectrum (to compare with experiments), one needs to account for the measurement setup as we show in the following section.

B. Detected emission

To be detected in a measurement, emitted light must be able to couple out from the photonic crystal and fall into the detector's aperture. In the photonic crystal, all modes are Bloch modes. Such a Bloch mode is able to couple to a plane wave mode in free space outside the photonic crystal if (a) the frequency ω is conserved and (b) the wave vector component $\boldsymbol{k}_{||}$ parallel to the specified interface is conserved [see Fig. 4(a)].

The latter criterion arises from translational symmetry[29] and should not be confused with Snell's law of refraction: looking at plane waves at an interface between homogenous materials, (b), in fact, yields Snell's law. In photonic crystals, however, there is no simple dispersion relation $\omega(\boldsymbol{k})$. Therefore it is necessary to look at $\boldsymbol{k}_{||}$, rather than at the angle of the wave vector inside the photonic crystal (in contrast to Ref. 8).

The out-coupling condition is thus $|\boldsymbol{k}_{||}| \leqslant \omega\sqrt{\epsilon_{\mathrm{out}}}/c$, where ϵ_{out} is the relative permittivity of the surrounding medium (e.g., air or immersion oil). Only part of the modes meet this criterion, the other modes are guided inside the photonic crystal (similar to total internal reflection).

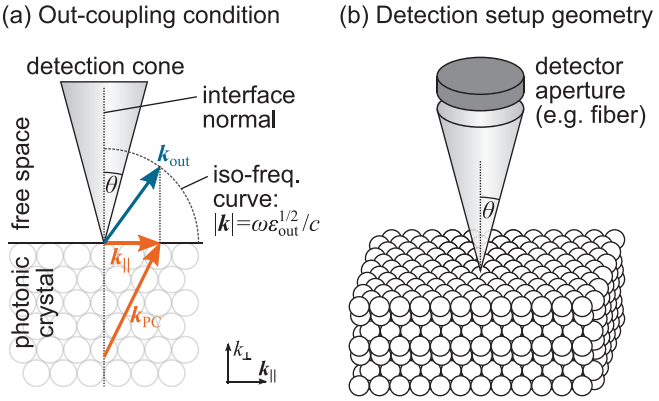

FIG. 4. (Color online) (a) Modes inside the photonic crystal can couple to plane waves in free space if the frequency ω and the wave vector component $\boldsymbol{k}_{||}$ parallel to the specific interface are conserved. To be detected, the wave vector $\boldsymbol{k}_0$ of the out-coupled wave must lie within the detection aperture. As an example, we calculate the detected spectrum for the measurement configuration shown in (b). The interface to air is formed by the {111} plane of the opal. Light is collected within a cone normal to the interface (half-angle θ).

Not all out-coupled modes, however, are detected by the measurement setup, only those that can be collected by the detection system. Here, we assume a setup with a cone of detection normal to the interface as illustrated in Fig. 4. Only modes whose wave vector lies within this cone are detected, which results in the condition

$$\left|\boldsymbol{k}_{||}\right| \leqslant \frac{\omega\sqrt{\epsilon_{\text{out}}}}{c}\sin(\theta), \tag{22}$$

where θ is the half-angle of the aperture. Of course, this condition can easily be adapted to other cases: e.g., a detection cone tilted to the sample surface at different angles could be used to study the angular characteristic of emitted light, which has been referred to as *angular* or *directional* redistribution.[8]

The detected spectrum can be calculated by restricting the LDOS analysis from Sec. II to modes that satisfy the detection condition. Thus we calculate the *fractional* LDOS (FLDOS) $\tilde{\rho}_{\text{f}}(\boldsymbol{r},\omega)$ analogous to Eq. (5), but only with the subset of modes in $\mathfrak{K}_{n,\omega}$ that satisfies Eq. (22). From this treatment we obtain the spectral shape function $g_{\text{f}}(\boldsymbol{r},\omega)$ of the detected spectrum from emission inside a photonic crystal:[33]

$$g_{\text{f}}^{\text{PC}}(\boldsymbol{r},\omega) = g^0(\omega)\frac{\gamma_{\text{f}}(\boldsymbol{r},\omega)}{\alpha_{\text{f}}(\boldsymbol{r})} \tag{23}$$

$$\text{with}\quad \alpha_{\text{f}}(\boldsymbol{r}) = \int g^0(\omega)\gamma_{\text{f}}(\boldsymbol{r},\omega)d\omega \tag{24}$$

$$\text{and}\quad \gamma_{\text{f}}(\boldsymbol{r},\omega) = \frac{\tilde{\rho}_{\text{f}}^{\text{PC}}(\boldsymbol{r},\omega)}{\tilde{\rho}_{\text{f}}^{0}(\boldsymbol{r},\omega)}, \tag{25}$$

where the corresponding FLDOS for emission in homogeneous media is $\tilde{\rho}_{\text{f}}^{0}(\boldsymbol{r},\omega) = \eta\,\tilde{\rho}^{0}(\boldsymbol{r},\omega)$ (due to the isotropic distribution of photon states). The factor η describes the fraction of modes that are detectable, thus depending on the measurement setup. For the detection cone in our example (see Fig. 4), we find $\eta = 1 - \cos[\arcsin(\sqrt{\epsilon_{\text{out}}/\epsilon}\,\sin\theta)]$ from geometric reasoning. Note that a weighted average analogous to Eq. (21) needs to be applied in case of multiple emitters at different locations.

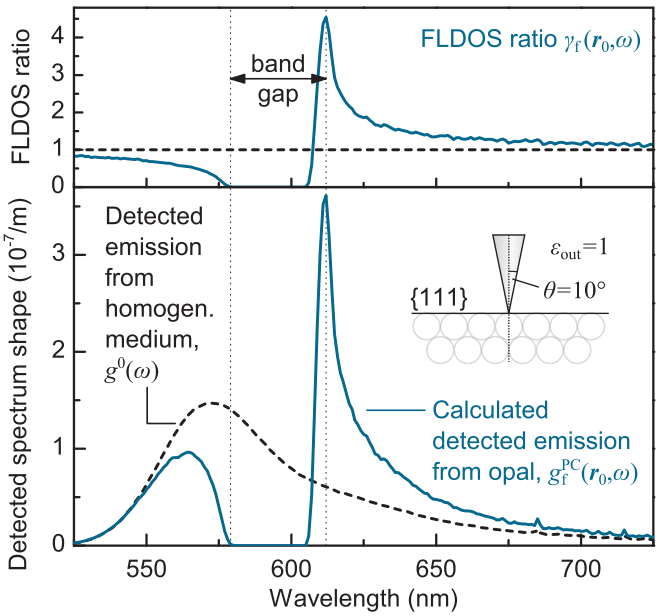

FIG. 5. (Color online) Restricting the LDOS analysis to detectable modes ($\theta = 10°$) changes the shape of the detected spectrum drastically: no light is detected within the band gap of the opal, which lies in the direction of the detection cone. Instead, a strong enhancement at the low-frequency band edge is found.

In Fig. 5, we plot the resulting spectral distribution of detected light of an emitter at $\boldsymbol{r}_0$ for a detection cone with half-angle $\theta = 10\ °$ (solid angle of 0.03π) normal to the typical {111} plane of the opal ($\epsilon_{\text{out}} = 1$).[41] The detected spectrum from the opal drastically differs from the undisturbed emission. Within the band gap, no light reaches the detector. No $\boldsymbol{k}$ vectors exist in this spectral region that fulfill Eq. (22). This would change if we widened the detection cone.

A strong enhancement is obtained at the low-frequency band edge arising from the elevated DOS at flat bands. The reason for the asymmetry of the FLDOS, i.e., the enhancement only on one edge of the band gap, is the spatial distribution of the fields: it is well known that modes at the lower band edge concentrate in the high-ϵ regions (*dielectric modes*) while the ones above the band gap have a larger fraction of their energy in the low-ϵ regions (*air modes*).[29] As we are looking at positions $\boldsymbol{r}$ within the spheres the (F)LDOS is enhanced at the low-frequency band edge. In fact, looking at $\boldsymbol{r}$ in the voids (air), we see the enhancement at the high-frequency band edge (not shown here).

The main message is, however, that the measured spectrum can differ very strongly from the spectral distribution of the totally emitted light, even in "weak" photonic crystals. The detected spectrum arises usually only from a small subset of all modes (here, $\eta = 0.7\%$). It can be more distorted in terms of suppressions due to band gaps and enhancements at band edges, when a band gap lies in the direction of detection. One can therefore not draw nonambiguous conclusions about the emitted spectrum from a measured spectrum. On the other side, predicting the detected spectrum from theory needs accurate knowledge of the exact measurement setup (detection aperture) and sample surface (to calculate the interface-parallel $\boldsymbol{k}_{||}$).

The result for the detected spectrum resembles the previously reported experimental results much better than the total emitted spectrum. Although the investigated systems differ (dye positions, measurement setup, etc.), our result qualitatively confirms the observation of a "dip" within the band gap.[8,20,21] But even when the exact same system is modeled and measured, the calculated and measured spectra can mismatch due to several reasons.

First, in our calculation we assumed that every mode, that is able to couple out, will couple out (i.e., with an efficiency of 100%). This is justified when light bounces between a top and bottom surface: with a nonzero out-coupling efficiency light will exit eventually at some point.

Further, modes of higher bands can have a set of different possibilities to couple out. Their $\boldsymbol{k}$ vectors are folded back into the FBZ, thus they may be able to couple to more than one plane wave mode outside the photonic crystal. This can be understood when the periodic interface is seen as a grating: light can therefore exit to different diffraction orders with different diffraction efficiencies. For the spectral range in our example, looking at the first band gap, this effect does not play a significant role. In other cases, however, it might be necessary to employ further calculations on the different out-coupling efficiencies.

On the other hand, imperfections in the experiment can cause differences between calculated and measured spectra: defects in the photonic crystal might scatter light in other directions, making it (un)detectable. Further, reabsorption of emitted light by other emitters may modify the measured spectrum. Finally, samples are always finite, whereas the calculations presented here are based on the assumption of infinite photonic crystals. Therefore emitters may have not enough periods/layers in their environment to establish the full LDOS effect, especially if positioned near surfaces.

The calculation of the detected spectrum is important for comparison with spectral measurements. Other experimentally accessible characteristics like the emitter quantum yield or the fluorescence lifetime, however, require consideration of all modes. The changes of these quantities induced by a photonic crystal are discussed in the following.

C. Emitter quantum yield

Besides spectral redistribution, the photonic crystal environment also affects the photoluminescence quantum yield of embedded emitters. The quantum yield Φ states the probability that a photon is emitted after one photon was absorbed and it is a key property of fluorescent materials. For the steady state ($\Gamma_{\mathrm{ABS}} = \Gamma_{\mathrm{SPE}} + \Gamma_{\mathrm{NRD}}$), we can write

$$\Phi = \frac{\Gamma_{\mathrm{SPE}}}{\Gamma_{\mathrm{ABS}}} = \frac{P_{\mathrm{SPE}}}{P_{\mathrm{SPE}} + P_{\mathrm{NRD}}}. \tag{26}$$

Applying this equation to both the homogeneous medium reference and the photonic crystal case, we find

$$\Phi^{\mathrm{PC}}(\boldsymbol{r}) = \frac{\alpha(\boldsymbol{r}) P^0_{\mathrm{SPE}}}{\alpha(\boldsymbol{r}) P^0_{\mathrm{SPE}} + P_{\mathrm{NRD}}} = \frac{\Phi^0 \alpha(\boldsymbol{r})}{1 + \Phi^0 \left(\alpha(\boldsymbol{r}) - 1\right)}. \tag{27}$$

Given the undisturbed emitter quantum yield Φ^0 of a fluorescent species in homogeneous media, the modified quantum yield in a photonic crystal environment can be described solely by the emission probability enhancement factor $\alpha(\boldsymbol{r})$, independent of the absorption process.

In our case study, we obtain a slight decrease in quantum yield from $\Phi^0 = 70\%$[42] to $\Phi^{\mathrm{PC}}(\boldsymbol{r}_0) = 69.7\%$ for the rhodamine B dye at position $\boldsymbol{r}_0$. This decrease is due to the overall slightly lower LDOS compared to the homogeneous medium [$\alpha(\boldsymbol{r}_0) = 0.987$]. With an LDOS larger than in the reference case the spontaneous emission rate would be increased and the quantum yield would be enhanced, as this radiative decay channel would be more favorable (compared to the nonradiative decay) than in the reference case.

Note that the emitter quantum yield inside the photonic crystal depends on the emitter location $\boldsymbol{r}$. To calculate the quantum yield of a group of emitters, the individual $\Phi^{\mathrm{PC}}(\boldsymbol{r}_i)$ needs to be averaged, weighted with the local absorption:

$$\Phi^{\mathrm{PC}}_{\mathrm{tot}} = \frac{\sum_i \Phi^{\mathrm{PC}}(\boldsymbol{r}_i)\, \beta(\boldsymbol{r}_i)}{\sum_i \beta(\boldsymbol{r}_i)}. \tag{28}$$

Further, we want to mention that the emitter quantum yield is not only affected by the LDOS. The chemical environment of the emitter may also have significant influence. It is therefore necessary to determine Φ^0 under the same chemical conditions as in the photonic crystal (same host material for embedding).

D. Fluorescence lifetime

In lifetime measurements, the decay of fluorescence is analyzed after the excitation has been turned off. The corresponding differential equation

$$\dot{N}_2(t) = -N_2(t)\,(P_{\mathrm{SPE}} + P_{\mathrm{NRD}}) \tag{29}$$

can be solved with the exponential ansatz $N_2(t) = N_2(0)\, e^{-t/\tau}$, where $\tau = (P_{\mathrm{SPE}} + P_{\mathrm{NRD}})^{-1}$ is called fluorescence lifetime.

Using Eq. (26), we can write $\tau = \Phi / P_{\mathrm{SPE}}$. Comparing the lifetime τ^{PC} inside a photonic crystal to the lifetime τ^0 in homogenous media, we find

$$\tau^{\mathrm{PC}}(\boldsymbol{r}) = \tau^0 \frac{1}{1 + \Phi^0\,[\alpha(\boldsymbol{r}) - 1]}. \tag{30}$$

This means that the relative change in fluorescence lifetime depends only on the quantum yield Φ^0 and the emission probability enhancement factor $\alpha(\boldsymbol{r})$ (which can be obtained through calculations of the LDOS). We want to emphasize the dependence on the quantum yield Φ^0: doing experiments with low-quantum yield emitters will result in very small changes in lifetime, even if the photonic crystal provides a large LDOS effect. This can be one reason for the small changes in lifetime reported in previous studies,[20–22] additional to small LDOS changes by the studied photonic crystals.

In our case study, we obtain $\tau^{\mathrm{PC}}(\boldsymbol{r}_0) = 1.009\,\tau^0$, i.e., a 0.9 % longer lifetime than in a homogeneous medium. For an emitter without nonradiative decay channels ($\Phi^0 = 1$), we would get a longer lifetime of $\tau^{\mathrm{PC}}(\boldsymbol{r}_0) = \tau^0/\alpha(\boldsymbol{r}_0) = 1.013\,\tau^0$. These results are in accordance with the reported observations of only little effect on the fluorescence decay in "weak" photonic crystals.

We want to point out that the measured fluorescence lifetime does not depend on the exact way of measuring it: it does not matter if luminescence is recorded only for specific wavelengths or integrated over the full spectrum,

nor if only part of the emitted light is detected in a certain measurement setup. The fractional transition probabilities might be different in these cases and therefore the absolute signal level.[33] The dynamics of the decay, however, depend only on the exponential decay of $N_2(t)$. This decay and thus the lifetime τ are determined by all possible transitions, not only those that are being monitored. This means that at the same time a strong modification of the spectrum (large FLDOS variation) but only little change in lifetime (small LDOS variation) may be observed, as shown for our opal example. Such behavior has been reported in previous experiments[20,21] and can now be explained with this reasoning.

When studying multiple emitters, the observed decay arises from the individual rates:

$$\Gamma^{\mathrm{PC}}_{\mathrm{tot}}(t) = \sum_i \Gamma^{\mathrm{PC}}_{\mathrm{SPE}}(\boldsymbol{r}_i)\, e^{-t/\tau^{\mathrm{PC}}(\boldsymbol{r}_i)} \approx \sum_i \frac{\Gamma^{0}_{\mathrm{SPE}}\, \alpha(\boldsymbol{r})\beta(\boldsymbol{r})}{1+\Phi^0[\alpha(\boldsymbol{r})-1]}\, e^{-t/\tau^{\mathrm{PC}}(\boldsymbol{r}_i)}. \quad (31)$$

Thus the decay becomes non-single-exponential. To calculate the contribution of each emitter, i.e., the pre-exponential factors, local absorption needs to be considered as well.

V. CONCLUSION

In conclusion, we have shown how to calculate the LDOS in photonic crystals from eigenmode computations. This method is very efficient and can be applied to arbitrary photonic crystals, such as the opal used as an example in this work.

By describing the electronic structure of a fluorescent emitter as a quasi-two-level system with appropriate spectral shape functions, we can assess the impact of the LDOS changes on the electronic transition probabilities according to Fermi's golden rule. As an example, we studied the emission of the dye rhodamine B. Our treatment, however, can be applied to all emitters whose electronic structure can be described in this way. For more complex emitters (e.g., several relevant electronic states), the rate equation model can be adapted.

With this approach, the emission spectrum inside a photonic crystal can be calculated, which can differ from the undisturbed spectrum due to spectral redistribution as a result of LDOS variations. In experiments, however, only part of the emitted light is measured. We demonstrated how to calculate the detected spectrum, given a specific setup geometry. This detected spectrum can strongly differ from the emitted spectrum, especially if a band gap exists in the direction of detection.

The absolute intensities of emitted and detected light depend on the absorption process, particularly on the local spectral energy density of the excitation. Although the treatment of the changes in excitation is out of the scope of this paper, we have shown how it influences the different transition rates. Independent from the absorption rate, however, the change in the emitter quantum yield in a photonic crystal environment can be calculated, i.e., how many of the absorbed photons are emitted.

Another property accessible in measurements is the fluorescence lifetime. We have calculated how this lifetime changes within a photonic crystal due to LDOS effects, depending on the emitter quantum yield (the smaller the quantum yield, the smaller the change in lifetime).

Both quantum yield and lifetime depend on the emission probability enhancement factor α, which is determined by the LDOS variation but also by the undisturbed emission spectrum (i.e., they depend on the emitter species). They do not depend on the measurement setup geometry. This insight explains why at the same time strong spectral modifications but small changes in lifetime were observed in previous experiments.

As multiple emitters at different positions in the photonic crystal experience different LDOS variations, we have obtained the aggregated emission spectrum, quantum yield and decay kinetics for a group of emitters. As a result, the (detected) spectra may be inhomogeneously broadened and the fluorescence decay becomes non-single-exponential.

With this work we provide a method for calculating the effects of a photonic crystal on the (detected) emission spectrum, the quantum yield, and the lifetime of fluorescent emitters. This allows quantitative comparison to experiments and helps to understand the physics behind the observations.

ACKNOWLEDGMENTS

The authors would like to thank Barbara Herter, Stefan Fischer and Sebastian Wolf from Fraunhofer ISE for fruitful discussions. The presented work was supported by the German Research Foundation (DFG) within the Nanosun II project (PAK88). Johannes Gutmann gratefully acknowledges the scholarship support from the Reiner Lemoine Stiftung. Jan Christoph Goldschmidt gratefully acknowledges the scholarship support from the German Academic Exchange Service (DAAD).

*johannes.gutmann@ise.fraunhofer.de

[1] E. M. Purcell, Phys. Rev. **69**, 674 (1946).
[2] E. Yablonovitch, Phys. Rev. Lett. **58**, 2059 (1987).
[3] S. John, Phys. Rev. Lett. **58**, 2486 (1987).
[4] V. Bykov, Soviet Physics JETP **35**, 269 (1972).
[5] J. P. Dowling and C. M. Bowden, Phys. Rev. A **46**, 612 (1992).
[6] K. Busch and S. John, Phys. Rev. E **58**, 3896 (1998).
[7] R. Wang, X.-H. Wang, B.-Y. Gu, and G.-Z. Yang, Phys. Rev. B **67**, 155114 (2003).
[8] M. Barth, A. Gruber, and F. Cichos, Phys. Rev. B **72**, 085129 (2005).
[9] I. S. Nikolaev, W. L. Vos, and A. F. Koenderink, J. Opt. Soc. Am. B **26**, 987 (2009).
[10] R. C. McPhedran, L. C. Botten, J. McOrist, A. A. Asatryan, C. M. de Sterke, and N. A. Nicorovici, Phys. Rev. E **69**, 016609 (2004).
[11] D. P. Fussell, R. C. McPhedran, and C. Martijn de Sterke, Phys. Rev. E **70**, 066608 (2004).
[12] S. J. Myers, D. P. Fussell, J. M. Dawes, E. Mägi, R. C. McPhedran, B. J. Eggleton, and C. M. de Sterke, Opt. Express **14**, 12439 (2006).

[13]W. L. Vos, A. F. Koenderink, and I. S. Nikolaev, Phys. Rev. A **80**, 053802 (2009).
[14]E. V. Hooijdonk, S. Berthier, and J.-P. Vigneron, J. Appl. Phys. **112**, 114702 (2012).
[15]E. V. Hooijdonk, C. Barthou, J. P. Vigneron, and S. Berthier, J. Opt. Soc. Am. B **29**, 1104 (2012).
[16]P. Bermel, A. Rodriguez, J. D. Joannopoulos, and M. Soljacic, Phys. Rev. Lett. **99**, 053601 (2007).
[17]B. Herter, S. Wolf, S. Fischer, J. Gutmann, B. Bläsi, and J. C. Goldschmidt, Opt. Express **21**, A883 (2013).
[18]M. J. A. de Dood, A. Polman, and J. G. Fleming, Phys. Rev. B **67**, 115106 (2003).
[19]S. G. Romanov, A. V. Fokin, and R. M. D. L. Rue, Appl. Phys. Lett. **76**, 1656 (2000).
[20]M. Megens, J. E. G. J. Wijnhoven, A. Lagendijk, and W. L. Vos, Phys. Rev. A **59**, 4727 (1999).
[21]E. P. Petrov, V. N. Bogomolov, I. I. Kalosha, and S. V. Gaponenko, Phys. Rev. Lett. **81**, 77 (1998).
[22]P. Lodahl, A. Floris van Driel, I. S. Nikolaev, A. Irman, K. Overgaag, D. Vanmaekelbergh, and W. L. Vos, Nature (London) **430**, 654 (2004).
[23]J. Li, B. Jia, G. Zhou, C. Bullen, J. Serbin, and M. Gu, Adv. Mater. **19**, 3276 (2007).
[24]M. R. Jorgensen, J. W. Galusha, and M. H. Bartl, Phys. Rev. Lett. **107**, 143902 (2011).
[25]M. D. Leistikow, A. P. Mosk, E. Yeganegi, S. R. Huisman, A. Lagendijk, and W. L. Vos, Phys. Rev. Lett. **107**, 193903 (2011).
[26]S. Ogawa, M. Imada, S. Yoshimoto, M. Okano, and S. Noda, Science **305**, 227 (2004).
[27]P. Vukusic and I. Hooper, Science **310**, 1151 (2005).
[28]J. Gutmann, J. Posdziech, M. Peters, L. Steidl, R. Zentel, H. Zappe, and J. C. Goldschmidt, Proc. SPIE **8438**, 84381O (2012).
[29]J. D. Joannopoulos, S. G. Johnson, J. N. Winn, and R. D. Meade, *Photonic Crystals - Molding the Flow of Light*, 2nd ed. (Princeton University Press, Princeton, New Jersey, 2008).
[30]S. G. Johnson and J. D. Joannopoulos, Opt. Express **8**, 173 (2001).
[31]G. Lehmann and M. Taut, Phys. Status Solidi B **54**, 469 (1972).
[32]J. Hama, M. Watanabe, and T. Kato, J. Phys.: Condens. Matter **2**, 7445 (1990).
[33]See Supplemental Material at http://link.aps.org/supplemental/10.1103/PhysRevB.88.205118 for additional information about the LDOS in homogenous media, further (L)DOS results, the effects of the LDOS on the line shape of individual transitions and fractional transition rates.
[34]In contrast, the LDOS within the voids (low permittivity) is strongly enhanced over its corresponding homogeneous LDOS, and the total DOS is, apart from band gaps, in good agreement with the DOS for an effective homogeneous material, as shown in Supplemental Material.[33]
[35]J. Lakowicz, *Principles of Fluorescence Spectroscopy* (Springer, London, 2009).
[36]K. Yee, IEEE Trans. Antennas Propag. **14**, 302 (1966).
[37]A. Taflove and S. C. Hagness, *Computational Electrodynamics: The Finite-Difference Time-Domain Method*, 3rd ed. (Artech House, Norwood, MA, 2005).
[38]M. G. Moharam and T. K. Gaylord, J. Opt. Soc. Am. **72**, 1385 (1982).
[39]D. M. Whittaker and I. S. Culshaw, Phys. Rev. B **60**, 2610 (1999).
[40]M. Fox, *Quantum Optics* (Oxford University Press, New York, NY, USA, 2006).
[41]For the calculation of the opal FLDOS, we increased the resolution of the grid in $\boldsymbol{k}$ space to $\Delta k = 0.005\ 2\pi/a$ to reduce binning noise. At the same time, we restricted the calculation to 1/8 of the FBZ to keep the computational effort reasonable.
[42]F. L. Arbeloa, P. R. Ojeda, and I. L. Arbeloa, J. Lumin. **44**, 105 (1989).